Long-Term Deactivation of Supported Pt Catalysts in the Dehydrogenation of Methylcyclohexane to Toluene

ARTICLE *in* INDUSTRIAL & ENGINEERING CHEMISTRY RESEARCH · SEPTEMBER 2010

Impact Factor: 2.59 · DOI: 10.1021/ie1013025

3 AUTHORS, INCLUDING:

Faisal AlHumaidan
Kuwait Institute for Scientific Research
21 PUBLICATIONS **135** CITATIONS
SEE PROFILE

Arthur Garforth
The University of Manchester
71 PUBLICATIONS **1,486** CITATIONS
SEE PROFILE

Long-Term Deactivation of Supported Pt Catalysts in the Dehydrogenation of Methylcyclohexane to Toluene

Faisal Alhumaidan,*,† David Cresswell,‡ and Arthur Garforth‡

Petroleum Research and Studies Center, Kuwait Institute for Scientific Research, P.O. Box 24885, Safat 13109, Kuwait, and Environmental Technology Center, School of Chemical Engineering and Analytical Science, The University of Manchester, P.O. Box 88, Sackville Street, Manchester M60 1QD, United Kingdom

The kinetics of methylcyclohexane (MCH) dehydrogenation over supported Pt catalysts was successfully described by a non-Langmuirian/noncompetitive Horiuti−Polanyi model (*Ind. Eng. Chem. Res.*, in press). The daily reversible and irreversible deactivation, associated with activity tests, was satisfactorily included in the dehydrogenation model. The objective of this work is to incorporate the long-term deactivation of Pt catalysts, associated with life or deactivation tests, in the kinetic model. This has been successfully achieved by assuming that the long-term deactivation is the sum of two exponential decay processes, one rapid and completed in a few days, while the other is slow with a half-life of weeks to months.

1. Introduction

Developing a catalyst that can maintain high stability requires a deep understanding of the deactivation phenomena. Groups of researchers have investigated the deactivation of Pt/Al_2O_3 catalysts in MCH dehydrogenation.[1–8] Some studies suggested that catalyst deactivation in MCH dehydrogenation is caused by two types of poison structures: one reversible and the other irreversible.[2–4] The reversible poison can be removed at normal operating temperature by a stream of pressurized hydrogen, whereas the irreversible poison cannot. The relative amount of each poison structure depends on the hydrogen partial pressure and the time "on-stream".

The investigation of the prolonged deactivation of Pt/Al_2O_3 catalyst in MCH dehydrogenation indicated two phases of deactivation.[2,5] The initial phase has a rapid rate and occurs over a relatively short period of time. This phase is also characterized by a comparatively low activation energy (33.4 kJ mol^{-1}) and is totally reversible in a stream of hydrogen. The second phase of deactivation, on the contrary, is characterized by a slower rate of deactivation, a high activation energy (163 kJ mol^{-1}), and partially reversible deactivation in a stream of hydrogen.

Pacheco and Petersen[6] proposed a deactivation mechanism and an empirical fouling correlation for the dehydrogenation of MCH. The fouling mechanism assumes an initial sequential adsorption of MCH on a group of six active sites (sextet). The series of dissociative adsorptions causes the MCH molecule to lose all 11 hydrogen atoms in its ring to form a multiply bound surface carbon skeleton. A hyperbolic deactivation function was proposed for this sextet fouling mechanism, which suggests that the fouling rate is directly proportional to MCH partial pressure and inversely related to hydrogen partial pressure. The sextet fouling mechanism fits the deactivation data quite well at a high level of catalyst activity but gradually deviates from the experimental data as the catalytic activity declines. This behavior suggests that a successful fouling model should not be based on a single reaction order but on a variable one to represent the fouling data over a wider range of catalyst activity.

The sextet fouling mechanism was modified to fit the fouling data over a wider range of catalyst activity.[7] To explain the discrepancy between fouling data and the sextet model at the lower range of activity, the modified fouling mechanism proposed that the fouling occurs on smaller multiplets as the sextets become exhausted. In other words, the initial deactivation mainly occurs on the sextet multiplet until the surface is depleted of that multiplet, then the fouling mechanism proceeds toward the five-sites multiplet and the process continues until it reaches the two-site multiplet (doublet fouling). The fouling reaction prefers the higher order multiplets because they have lower fouling activation energy. Pacheco and Petersen[7] reported that the initial rate of the sextet fouling is 1000 times faster than that of doublet fouling.

Another mechanism for Pt/Al_2O_3 deactivation in MCH dehydrogenation was proposed by Chai and Kawakami.[8] The mechanism suggested that methylcyclohexadiene, formed as an intermediate, is adsorbed in a different way from that in the main reaction to form a coke precursor. The polymerization of "n" adjacently adsorbed precursors is assumed to be the rate-controlling step of the deactivation reaction. The parameter "n" in this deactivation model can be interpreted in different ways such as the number of adjacently adsorbed coke precursor molecules, the number of active sites involved in the coke formation, or the order of the deactivation reaction. Chai and Kawakami[8] reported that the value of "n" falls between 2.6 and 2.8 for a Pt/Al_2O_3 catalyst. Corma et al.[9] similarly reported that "n" is equal to 3 in the dehydrogenation of MCH over Pt−NaY catalyst.

An impressive extension of the life of a monometallic Pt/Al_2O_3 catalyst was achieved in 1968 by adding Re to form a bimetallic reforming catalyst.[10,11] Scientists proposed different rational explanations to justify this fundamental catalysis phenomenon that has significantly advanced many conversion processes.[12–19]

In a previous work, the kinetic of MCH dehydrogenation over monometallic and bimetallic Pt catalysts was described by the non-Langmuirian/noncompetitive Horiuti−Polanyi (H−P) dehydrogenation model.[1] The daily reversible and irreversible deactivation was successfully included in this model. The objective of this work is to further validate the kinetic model by incorporating the long-term deactivation associated with MCH dehydrogenation over Pt catalysts.

* To whom correspondence should be addressed. E-mail: fhumaidan@prsc.kisr.edu.kw.
† Kuwait Institute for Scientific Research.
‡ The University of Manchester.

10.1021/ie1013025
Published on Web 09/15/2010

Table 1. Ranges of Operating Conditions of the Activity Tests

operating variable	unit	value range
temperature	°C	340−450
pressure	bar	1−9
MCH flow rate	mL h^{-1}	7.5−30
H_2 flow rate	NL min^{-1}	0−800
H_2/MCH		0−9
W/F	g s (mol MCH)$^{-1}$	3.06×10^4 to 1.224×10^5

Table 2. Operating Conditions of the Life Tests

operating variable	unit	value
temperature	°C	380
pressure	bar	1
MCH flow rate	mL h^{-1}	7.5
H_2 flow rate	NL min^{-1}	0
H_2/MCH		0
W/F	g s (mol MCH)$^{-1}$	1.224×10^5

2. Experimental Section

2.1. Apparatus. Two types of catalytic tests have been performed: activity tests and life tests. The deactivation observed in the activity tests is referred to as the "short-term" deactivation, while that associated with the life tests is called "long-term" deactivation. The activity tests were performed within a high-pressure stainless steel reactor, while the life tests were conducted on a similar glass reactor at atmospheric pressure. The schematic diagram of the apparatus is illustrated in Alhumaidan et al.,[1] while the design specification is given in Alhumaidan.[20]

2.2. Activity Tests. Each activity test consists of four runs that have been performed at fixed operating temperature and pressure, but different flow rates of MCH and/or H_2. The MCH flow rates for the first three runs were 7.5, 15, and 30 mL h^{-1}, respectively. The fourth run, on the other hand, is a repeat of the first run to assess the extent of catalyst deactivation at the end of each experiment. The hydrogen flow rate could be also varied. In some experiments, the hydrogen flow rate was held constant, and in others it was varied to maintain the H_2/MCH molar ratio fixed at 9. The ranges of operating variables of the activity tests are given in Table 1.

2.3. Life Tests. Deactivation tests were conducted in this study to evaluate the stability of catalysts. Seven deactivation tests have been conducted, which covers all catalysts investigated in this research. The operating conditions of the life tests are shown in Table 2, and each test ran continuously for approximately 600 h (25 days). In the first 10 h of the test, a sample was collected every 2 h to observe the initial phase of deactivation. After that, a sample was collected every 24 h.

2.4. Sample Analysis. All liquid samples were analyzed by gas chromatography (GC) to determine the MCH conversion at various conditions. The GC was a Varian (model-3400), equipped with a BP-5 capillary column (50 m × 0.25 mm i.d., 5% phenyl and 95% Ddimethylpolysiloxane, termed nonpolar) and flame ionization detector (FID). To closely investigate the effect of byproduct on catalyst stability, selected samples were analyzed by gas chromatography−mass spectroscopy (GC−MS), Agilent Technologies (model-6890N), equipped with an HP-5MS capillary column (50 m × 0.25 mm i.d., 5% phenyl and 95% methylpolysiloxane, termed nonpolar). Standard samples were prepared for the GC and the GC−MS analyses to permit quantitative determinations of reactant conversion and product yields and allow periodic checks for changes in the detector sensitivity.

2.5. Catalyst. Prototype monometallic and bimetallic Pt catalysts were prepared and compared to some commercially available ones in a fixed-bed reactor under operating conditions previously indicated in Tables 1 and 2. A general characterization of these catalysts is shown in Table 3, while the preparation details, detailed characterization, and catalyst loading and activation are given in previous work.[1,20]

3. Results and Discussion

In a previous paper,[1] various kinetic models were developed for MCH dehydrogenation over supported Pt catalysts. The best fitting mechanistic model was of the non-Langmuirian/noncompetitive Horiuti−Polanyi type. In this model, the Horiuti−Polanyi aromatic hydrogenation mechanism,[21−26] which assumes an atomic hydrogen addition to aromatics on the catalyst surface, was applied in reverse to MCH dehydrogenation. The model also assumed that hydrogen and MCH molecules adsorb on two different types of site (noncompetitive) to accommodate the observed near zero-order dependence of reaction rate on MCH and the negative order dependence upon hydrogen. To account for the increase in the hydrogen inhibition effect with pressure, a non-Langmuirian adsorption isotherm was adopted, which assumes a nonlinear dependency between the adsorption equilibrium constant for hydrogen and pressure. The short-term deactivation, associated with the activity tests, was satisfactorily included in the non-Langmuirian/noncompetitive Horiuti−Polanyi (H−P) dehydrogenation model.[1] The objective of this work is to successfully account for the long-term deactivation in this kinetic model. Before the "long-term" deactivation is addresses, a brief summary of the previously modeled short-term deactivation is presented.

3.1. Short-Term Deactivation. The short-term deactivation accounts for both daily and cumulative deactivation observed in the activity tests. The daily deactivation represents the extent of drop in activity over a one day experiment, while the cumulative deactivation is the sum of all irreversible deactivations of daily experiments. The extent of the loss of conversion for the daily deactivation was observed by a repeat run at the end of each experiment, while the extent of cumulative deactivation was determined by carrying out repeat experiments over longer time intervals. The daily deactivation was largely reversible by overnight reduction under hydrogen, while the cumulative deactivation was mostly irreversible by reduction. The short-term deactivation has been empirically determined by introducing two time scales into the apparent rate constant to account for the daily and cumulative deactivation.[1] Thus, the apparent rate constant was written as:

Table 3. Catalyst Properties

catalyst	symbol	supplier	metal loading (wt %)	metal dispersion	preparation technique	particle size (mm)	BET surface area (m^2/g)	pore volume (cm^3/g)	average pore diameter (Å)
$Pt_{1.0}/\gamma$-Al_2O_3	Pt1.0 (C)	commercial	Pt = 1	uniform	N/A	0.5−0.8	302	0.52	67
$Pt_{0.5}/\gamma$-Al_2O_3	Pt0.5 (C)	commercial	Pt = 0.5	egg-shell	N/A	1	125	0.35	110
$Pt_{1.0}/\gamma$-Al_2O_3	Pt1.0	prototype	Pt = 1	uniform	wet impregnation	0.5−0.8	220	0.62	70
$Pt_{0.3}/\gamma$-Al_2O_3	Pt0.3	prototype	Pt = 0.3	uniform	wet impregnation	0.5−0.8	220	0.62	70
$Pt_{0.3}$−$Re_{0.3}/\gamma$-Al_2O_3	Pt−Re (sq)	prototype	Pt = 0.3, Re = 0.3	uniform	sequential impreg. (sq)	0.5−0.8	220	0.62	70
$Pt_{0.3}$−$Re_{0.3}/\gamma$-Al_2O_3	Pt−Re (co)	prototype	Pt = 0.3, Re = 0.3	uniform	co-impregnation (co)	0.5−0.8	220	0.62	70
$Pt_{0.3}$−$Pd_{0.3}/\gamma$-Al_2O_3	Pt−Pd	prototype	Pt = 0.3, Pd = 0.3	uniform	co-impregnation	0.5−0.8	220	0.62	70

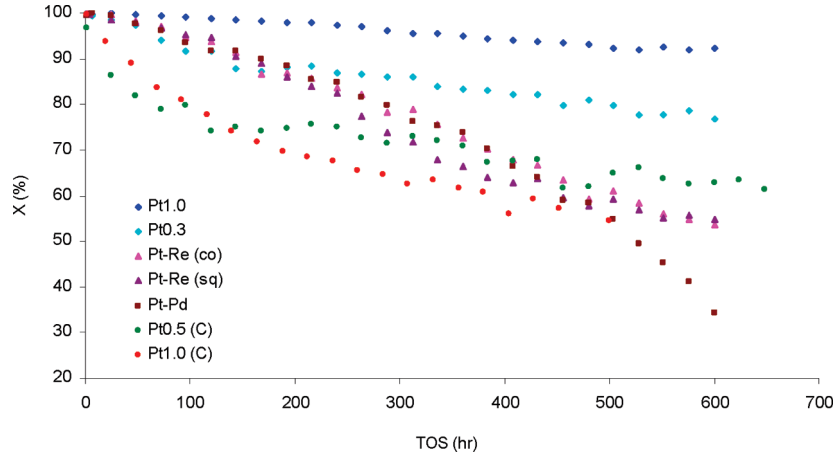

Figure 1. Long-term deactivation results. The tests were conducted at 380 °C, 1 bar, W/F = 1.224×10^5 g s mol^{-1}, and H_2/MCH = 0 in feed.

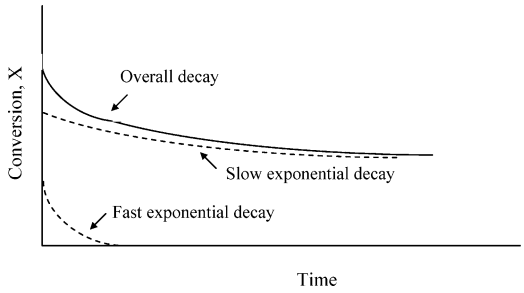

Figure 2. Overall deactivation curve consists of two phases of deactivation: fast and slow exponential decays.

$$k = k_o \cdot \exp(-k_d \cdot t_d) \cdot \exp(-k_c \cdot t_c) \quad (1)$$

where k_d and k_c are the rate constants for daily and cumulative deactivation, respectively. The daily deactivation rate constant (k_d) was obtained by incorporating a time-dependent factor into a simple power-law model. It was found that k_d is a strongly decreasing function of the total pressure (P), although the particular relationship is catalyst dependent. The rate constant of cumulative or irreversible deactivation, on the other hand, was determined by fitting the kinetic data to the non-Langmuirian/noncompetitive H−P model, which indicates negligible irreversible deactivation ($k_c = 0$) for the majority of catalysts.[1]

3.2. Long-Term Deactivation. The long-term performance of the commercial and the prototype catalysts was determined by conducting a life test on each catalyst. The results of the life tests are illustrated in Figure 1. The overall deactivation pattern in the vast majority of catalysts tested is apparently made up of two underlying exponential decay curves, as shown in Figure 2. The fast decay curve is often called the initial phase of deactivation, which is characterized by a rapid rate of deactivation over a relatively short period of time. The slow decay curve, on the other hand, represents the second phase of deactivation and is often referred to as the plateau. The plateau is characterized by a slow and consistent rate of deactivation and takes many weeks or months to decay to zero. The observed deactivation pattern suggests that the MCH dehydrogenation reaction occurs simultaneously on two independent populations of sites: one is subject to rapid deactivation, while the other is much more resistant to deactivation.

Two approaches have been considered to analyze the long-term deactivation. The first approach is based on an empirical fit to the deactivation data, which determines the population of the two types of active sites and their decay constants. In the second approach, a deactivation kinetic model is developed based on the non-Langmuirian/noncompetitive H−P kinetic model.

3.2.1. Empirical Curve-Fit to the Deactivation Data. The two-phase deactivation pattern observed over the majority of tested catalysts can be accounted for by fitting the deactivation data to two independent decay functions. The fitting of the deactivation data (by TableCurve-2D Software) indicates that the best-fit is achieved by using two exponential decay functions, as illustrated in eq 2. In this equation, X represents the observed conversion, t is the time-on-stream, and a, b, c, and d are empirical constants.

$$X = a \cdot \exp(-b \cdot t) + c \cdot \exp(-d \cdot t) \quad (2)$$

The first exponential decay term in eq 2 represents the fast initial deactivation, while the second exponential term corresponds to the slow and longer lived deactivation process. Both deactivation processes are described by the first-order deactivation function $f(t) = i \cdot \exp(-j \cdot t)$, where i represents the population of the active sites and j is the decay constant of that active site. Therefore, we may say that the empirical correlation parameters of eq 2 exemplify the following: a, the population of the rapidly deactivated sites; b, first-order decay constant of the rapidly deactivated sites (h^{-1}); c, the population of the slowly deactivated sites; and d, first-order decay constant of the slowly deactivated sites (h^{-1}).

Fitting the deactivation data of the various catalysts by the double exponential decay function gives the results shown in Table 4. The results for the Pt−Pd catalyst were not reported in Table 4 because the double exponential decay does not fit the catalyst deactivation pattern. On the basis of this empirical analysis, we may say that the rapidly deactivated site population in commercial Pt1.0(C) catalyst is approximately 23.5% of total

Table 4. Results of Fitting the Deactivation Curves by the Sum of Two Independent Exponential Decay Functions

catalyst	supplier	symbol	a	b	c	d	b/d	R^2
$Pt_{1.0}/Al_2O_3$	commercial	Pt1.0 (C)	23.42	0.01112	76.39	0.00066	17	0.9945
$Pt_{0.5}/Al_2O_3$	commercial	Pt0.5 (C)	16.20	0.04150	81.11	0.00044	94	0.9565
$Pt_{1.0}/Al_2O_3$	prototype	Pt1.0	8.67	0.00016	91.77	0.00015	1	0.9786
$Pt_{0.3}/Al_2O_3$	prototype	Pt0.3	7.14	0.01407	93.31	0.00032	44	0.9835
$Pt_{0.3}-Re_{0.3}/Al_2O_3$	prototype	Pt−Re(co)	59.68	0.00101	43.79	0.00104	1	0.9796
$Pt_{0.3}-Re_{0.3}/Al_2O_3$	prototype	Pt−Re(sq)	73.17	0.00114	30.59	0.00114	1	0.9785

Table 5. Results of Fitting the Deactivation Curves with a Single Exponential Function

catalyst	supplier	symbol	a	b	R^2
$Pt_{1.0}/Al_2O_3$	prototype	Pt1.0	100.44	0.00015	0.9786
$Pt_{0.3}-Re_{0.3}/Al_2O_3$	prototype	Pt−Re(co)	103.47	0.00103	0.9796
$Pt_{0.3}-Re_{0.3}/Al_2O_3$	prototype	Pt−Re(sq)	103.75	0.00114	0.9785

Table 6. Results of Fitting the Pt−Pd Deactivation Curves by the 1/2 Order Decay Function

catalyst	supplier	symbol	a	b	R^2
$Pt_{0.3}-Pd_{0.3}/Al_2O_3$	prototype	Pt−Pd	105.25	0.01121	0.9785

active sites, while the slowly deactivated site population is around 76.5%. The ratio b/d for Pt1.0(C) suggests that the rapidly deactivated sites deactivate 17 times faster than the slowly deactivated sites. Similarly, the rapidly deactivated sites represent 16.6% of the total active sites in the commercial Pt0.5(C) catalyst, while the slowly deactivated sites represent 83.4%. The deactivation rate of the rapidly deactivated sites in Pt0.5(C) is 94 times faster than that of the slowly deactivated sites. Figure 1 indicates that the stabilities of these two commercial catalysts, Pt1.0(C) and Pt0.5(C), were inferior to the prototype monometallic catalysts. The main reason for the low stability is the steep initial deactivation, which results in a substantial loss of catalyst activity in the plateau. To overcome this limitation and to operate at relatively higher activity, the duration and the steepness of the initial deactivation need to be reduced. This can be achieved by optimizing the empirical correlation parameters, where ideally one would desire $c \gg a$ and $d \ll b$. This modification in the empirical parameters has been partially fulfilled with the in-house Pt0.3 catalyst and results in significant improvements in catalytic activity and stability.

For the prototype Pt1.0 and Pt−Re (co and sq) catalysts, the rapidly deactivated sites and the slowly deactivated sites showed similar rates of deactivation ($b/d = 1$), which suggest a single population of active sites. Thus, the decay curves of these catalysts may be well fitted by the single exponential function:

$$X = a \cdot \exp(-b \cdot t) \tag{3}$$

where a is the population of all active sites, and b is the first-order decay constant of all active sites (h^{-1}).

Fitting the deactivation curves of these three catalysts by eq 3 gives the results illustrated in Table 5.

The most stable of all catalysts tested was observed in the prototype Pt1.0 catalyst. This is mainly due to the absence of a sharp initial deactivation and the very low deactivation rate in the plateau. The decay constant "b" of Pt1.0 has the lowest value among all catalysts, and it is at least an order of magnitude lower than that of the bimetallic catalysts. For the Pt−Re catalysts, Figure 1 and Table 5 suggest that the difference in preparation techniques (co- and sequential impregnation) did not significantly affect the rate of deactivation.

The deactivation trend of the Pt−Pd catalyst shows a steep deactivation following upon a 1/2 order decay pattern:

$$X = \left(a - a^{1/2} \cdot b \cdot t^{1/2} + \frac{b^2 \cdot t^2}{4}\right) \tag{4}$$

where a is the population of all active sites, and b is the 1/2 order decay constant of all active sites ($h^{-1/2}$).

The result of fitting the deactivation curve of Pt−Pd by eq 4 is given in Table 6. The deactivation constant "b" of the Pt−Pd catalyst is 2 orders of magnitude greater than that of the slow step "d" of the commercial and prototype monometallic catalysts and 1 order of magnitude higher than that of prototype Pt−Re catalysts.

It is important to note at this stage that the illustrated deactivation pattern is only valid under the given operating conditions of the life tests. However, the deactivation patterns are expected to be totally different at elevated pressure based on the short-term deactivation observed in the activity tests.[1]

3.2.2. Kinetic Model for the Long-Term Deactivation. The short-term deactivation was successfully included in the non-Langmuirian/noncompetitive H−P kinetic model for MCH dehydrogenation by introducing two time scales into the apparent rate constant to account for the daily and cumulative deactivations. The intention now is to introduce the long-term deactivation effect into the kinetic model. The initial reaction rate for the non-Langmuirian/noncompetitive H−P model[1] was given by:

$$(-r_1)_o = \frac{k}{(1 + K_3^{0.5} \cdot p_{3,o}^{0.5})} \tag{5}$$

where k is the reaction rate constant (mol g^{-1} s^{-1}), K_3 is the adsorption equilibrium constant for hydrogen (bar^{-1} H_2), and $p_{3,o}$ is the hydrogen partial pressure in the feed (bar). However, because the feed in the life test experiments was pure MCH (no hydrogen was added), the initial reaction rate becomes:

$$(-r_1)_o = k \tag{6}$$

The empirical fit of the experimental data indicated that the deactivation curve can be accurately fitted by the sum of two independent exponential decay functions. Therefore, the apparent rate constant may be written as:

$$k = k_1 \cdot \exp(-b_1 \cdot t) + k_2 \cdot \exp(-b_2 \cdot t) \tag{7}$$

where k_1 and k_2 are the rate constants for the fast and slow deactivation processes (mol g^{-1} s^{-1}), while b_1 and b_2 are their respective decay (h^{-1}). At $t = 0$, the rate constant becomes $k = k_o = k_1 + k_2$. The apparent rate constants k_1 and k_2 might be written as:

Table 7. Results Summary for the Kinetics Model of Long-Term Deactivation

catalyst symbol	modeling parameters	best-fit value	unit	std error	statistical parameters
Pt1.0 (C)	$k_1 \times 10^5$	1.8730	mol g^{-1} s^{-1}	0.1561	$R^2 = 0.9969$
	$k_2 \times 10^5$	1.2353	mol g^{-1} s^{-1}	0.0330	SSR = 0.0010
	b_1	0.0229	h^{-1}	0.0020	std dev = 0.0077
	b_2	0.0013	h^{-1}	0.0001	$F = 1830$
Pt0.5 (C)	$k_1 \times 10^5$	1.4333	mol g^{-1} s^{-1}	0.4099	$R^2 = 0.9556$
	$k_2 \times 10^5$	1.3193	mol g^{-1} s^{-1}	0.0345	SSR = 0.0082
	b_1	0.0560	h^{-1}	0.0151	std dev = 0.0185
	b_2	0.0008	h^{-1}	0.0001	$F = 172$
Pt1.0	$k_1 \times 10^5$	3.5934	mol g^{-1} s^{-1}	0.4155	$R^2 = 0.9922$
	$k_2 \times 10^5$	1.8994	mol g^{-1} s^{-1}	0.6472	SSR = 0.0002
	b_1	0.0053	h^{-1}	0.0016	std dev = 0.0027
	b_2	0	h^{-1}	0.0004	$F = 1016$
Pt0.3	$k_1 \times 10^5$	3.9226	mol g^{-1} s^{-1}	1.4505	$R^2 = 0.9892$
	$k_2 \times 10^5$	2.0445	mol g^{-1} s^{-1}	0.0438	SSR = 0.0015
	b_1	0.0319	h^{-1}	0.0065	std dev = 0.0079
	b_2	0.0009	h^{-1}	0.0001	$F = 733$
Pt−Re (co)	$k_1 \times 10^5$	2.4963	mol g^{-1} s^{-1}	0.9029	$R^2 = 0.9957$
	$k_2 \times 10^5$	2.4750	mol g^{-1} s^{-1}	0.1364	SSR = 0.0029
	b_1	0.0171	h^{-1}	0.0048	std dev = 0.0110
	b_2	0.0024	h^{-1}	0.0001	$F = 1873$
Pt−Re (sq)	$k_1 \times 10^5$	3.9148	mol g^{-1} s^{-1}	0.2236	$R^2 = 0.9969$
	$k_2 \times 10^5$	0.5862	mol g^{-1} s^{-1}	0.2144	SSR = 0.0022
	b_1	0.0070	h^{-1}	0.0009	std dev = 0.0098
	b_2	0	h^{-1}	0.0005	$F = 2457$

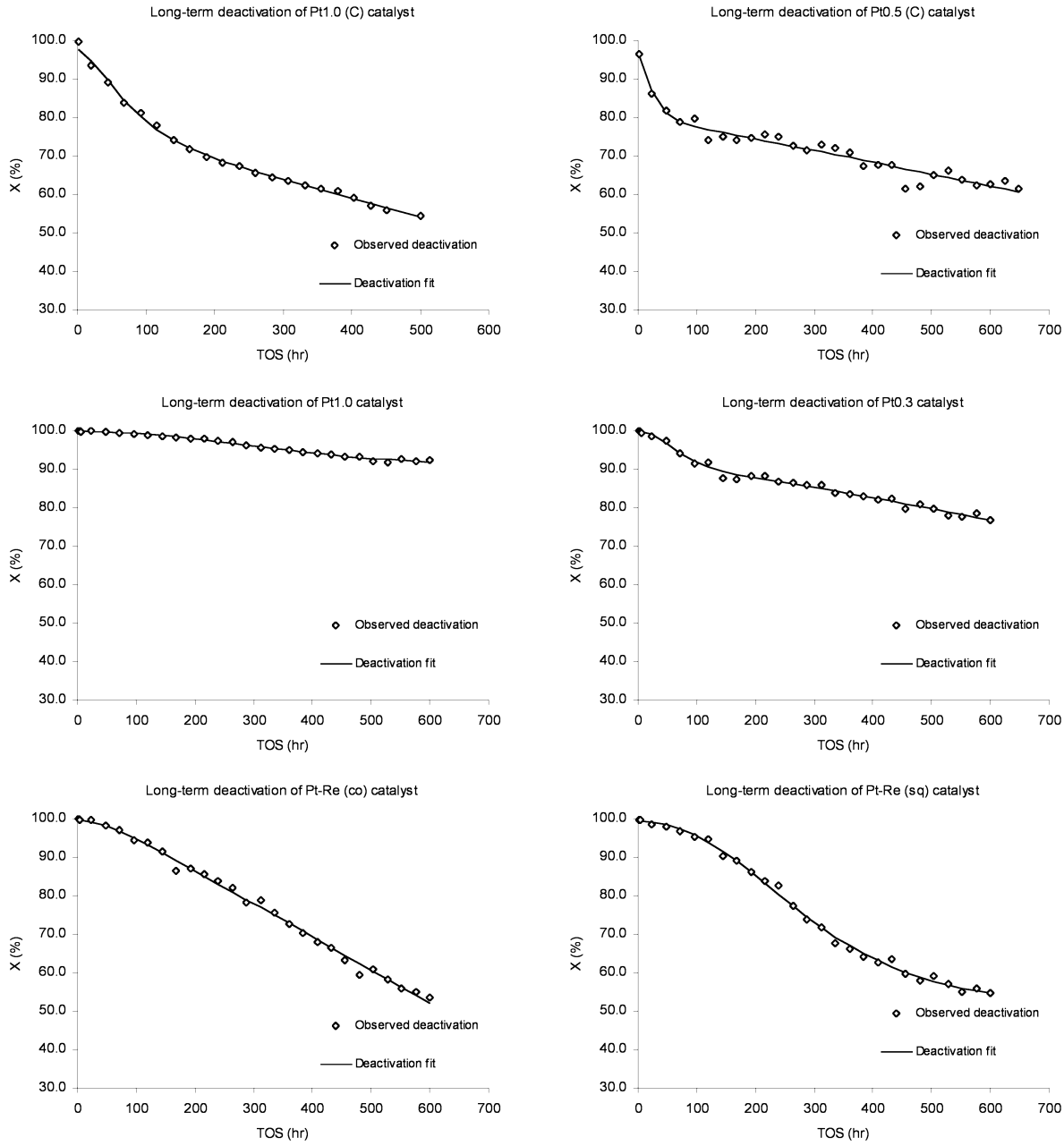

Figure 3. Fitting the deactivation data of tested catalysts by the double exponential decay model.

$$k_1 = k_1' \cdot A_1 \tag{8}$$

$$k_2 = k_2' \cdot A_2 \tag{9}$$

where k_1' is the intrinsic rate constant for type 1 sites [mol (m^2 Pt)$^{-1}$ s^{-1}], A_1 is the Pt area for type 1 sites [(m^2 Pt) (g catalyst)$^{-1}$], k_2' is the intrinsic rate constant for type 2 sites [mol (m^2 Pt)$^{-1}$ s^{-1}], and A_2 is the Pt area for type 2 sites [(m^2 Pt) (g catalyst)$^{-1}$].

In the deactivation tests, it is k_1 and k_2 that are determined. On the other hand, it is $k = k_1 + k_2$ that is determined in the activity tests. To determine k_1' and k_2', we need to have some means of determining A_1 and A_2. It is possible, therefore, that a high value of k_1 is the product of a very high value of k_1' and a small value of A_1 (i.e., very active sites "s_1", but a small population), or is the product of a small value of k_1' and high value of A_1 (i.e., relatively inactive but abundant "s_1" sites). It is impossible to say from the data that the "s_1" sites, which decay rapidly, are highly active, while "s_2" sites, which decay more slowly, are less active.

The observed conversion in the non-Langmuirian/noncompetitive H−P model[1] was given as:

$$X_{obs} = X_e \cdot \left[1 - \exp\left(\frac{-x \cdot (-r_1)_o}{X_e}\right)\right] \tag{10}$$

where X_{obs} is the observed conversion, X_e is the equilibrium conversion, and x is $(W/F_{1,o}) \times 10^{-5}$. At the given operating conditions of the life tests (T = 380 °C, P = 1 bar, W/F = 1.224×10^5 g s mol^{-1}, and H_2/MCH = 0 in the feed), the reaction is essentially irreversible, and the equilibrium conversion happens to be very close to one ($X_e \approx 1$). Therefore, the observed conversion may be written as:

$$X_{obs} = 1 - \exp(-x \cdot (-r_1)_o) \tag{11}$$

By substituting eqs 6 and 7 into eq 11 and fitting the deactivation data, the kinetic parameters of the long-term deactivation can

Table 8. Comparison between Stability Parameters for the Tested Catalysts

catalyst symbol	$k_o \times 10^5$ (g mol g^{-1} s^{-1})	k_1/k_o	k_2/k_o	b_1 (h^{-1})	b_2 (h^{-1})
Pt1.0 (C)	3.1083	0.6026	0.3974	0.0229	0.0013
Pt0.5 (C)	2.7526	0.5207	0.4793	0.0560	0.0018
Pt1.0	5.4928	0.6542	0.3458	0.0053	0
Pt0.3	5.9671	0.6574	0.3426	0.0319	0.0009
Pt−Re (co)	4.9713	0.5021	0.4979	0.0171	0.0024
Pt−Re (sq)	4.5010	0.8697	0.1303	0.0070	0

Table 9. Fitting the Kinetic Data Using a Single Exponential Decay Function

catalyst symbol	modeling parameters	best-fit value	unit	std error	statistical parameters
Pt1.0					$R^2 = 0.9406$
	$k_o \times 10^5$	3.8991	mol g^{-1} s^{-1}	0.1319	SSR = 0.0013
	b	0.0012	h^{-1}	0.0001	std dev = 0.0072
					$F = 411$
Pt−Re (co)					$R^2 = 0.9856$
	$k_o \times 10^5$	2.9316	mol g^{-1} s^{-1}	0.1029	SSR = 0.0098
	b	0.0027	h^{-1}	0.0001	std dev = 0.0194
					$F = 1776$
Pt−Re (sq)					$R^2 = 0.9538$
	$k_o \times 10^5$	2.6685	mol g^{-1} s^{-1}	0.1604	SSR = 0.0327
	b	0.0027	h^{-1}	0.0002	std dev = 0.0361
					$F = 516$

be determined. The results of fitting this kinetic model to the deactivation data are illustrated in Table 7 and Figure 3. The statistical parameters of Table 7 are previously defined in Alhumaidan et al.[1] Again, the result for the Pt−Pd catalyst was not included in the table because its deactivation pattern does not fit the double-exponential decay function.

To effectively compare the stability of catalysts, we need to consider various kinetic parameters such as the rate constant of the initial deactivation phase (k_1), the rate constant of the plateau phase (k_2), the initial rate constant for the whole deactivation process ($k_o = k_1 + k_2$), the proportion between the two deactivation phases (k_1/k_o and k_2/k_o), and the decay constants for the two deactivation phases (b_1 and b_2). Note that k_1/k_o represents the proportion of activity obtained from the rapidly deactivated sites (s_1), while k_2/k_o exemplifies the fractional activity obtained from the slowly deactivated sites (s_2). A highly stable dehydrogenation catalyst is characterized by high k_o, low k_1/k_o, high k_2/k_o, and low b_1 and b_2. These stability parameters have been compared for the tested catalysts in Table 8. The most important observations in Table 8 and Figure 3 are as follows:

(1) The values of the initial rate constant k_o suggest that Pt0.3 has the highest initial activity followed by Pt1.0. The catalyst with the lowest initial activity, on the other hand, is Pt0.5 (C) followed by Pt1.0 (C). The life test observations with regard to initial activity are in agreement with the observations noted previously from the activity tests.[1]

(2) 60% of the initial activity of Pt1.0(C) is lost in the fast initial deactivation. Similarly, 65% of the initial activity in the prototype Pt1.0 catalyst was consumed in the initial deactivation. However, the prototype Pt1.0 catalyst shows superior long-term activity. This is mainly due to the higher initial activity k_o (approximately 57% higher than that of Pt1.0(C)) and the slower decay rate particularly in the slow decay phase. The apparent zero decay rate of the plateau phase for the prototype Pt1.0 catalyst suggests that a much longer deactivation period is needed before an accurate estimate of the very low deactivation rate can be made.

(3) 65.7% of the total activity for Pt0.3 was destroyed in the initial phase of deactivation, while 34.3% of that activity remained for the plateau deactivation. In other words, 2/3 of the total activity was consumed in the first 100 h of operation, while 1/3 remained for the remaining 500 h. If these activity

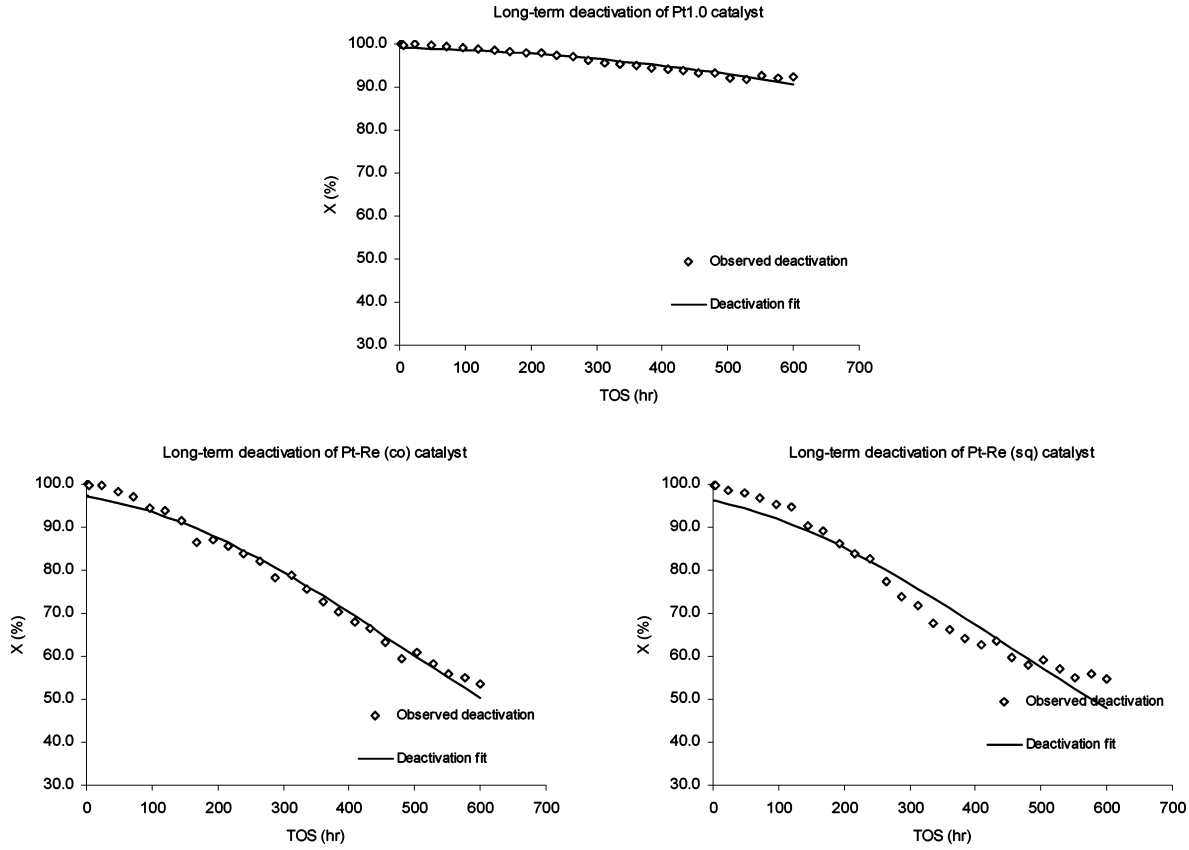

Figure 4. Fitting the deactivation data of prototype Pt1.0, Pt−Re (co), and Pt−Re (sq) catalysts by the single exponential decay model.

trends could be reversed, and thus 65.7% of total activity is preserved for the second phase of deactivation, then the catalyst would operate at substantially higher activity for longer time. Achieving this objective requires the identification of the key factors that determine k_1 and k_2 (nature of s_1 and s_2 sites). In other words, one needs to identify the factors that determine the population of the sites (area A_1 and A_2 per unit mass), and their intrinsic activities k_1' and k_2' (g mol/s m^2 site s_1, and g mol/s m^2 site s_2).

(4) The sequential impregnation decreased the initial activity (k_o) in the Pt−Re (sq) catalyst. This might be attributed to the coverage of some Pt sites by Re atoms, which eventually reduce the total Pt surface area. The lower initial activity in Pt−Re (sq) was compensated by relatively lower decay constants as compared to the Pt−Re (co). These two factors combined might explain the observed similarity in deactivation pattern between the two Pt−Re catalysts.

The empirical fitting of the data and the results obtained from the kinetic model suggest that the prototype Pt1.0 and Pt−Re catalysts can be fitted by a single exponential decay function:

$$k = k_o \cdot \exp(-b \cdot t) \tag{12}$$

where k_o is the initial rate constant and b is the decay constant. The results of fitting the long-term deactivation data by the single exponential decay are given in Table 9. The quality of fit for the single exponential decay function, as illustrated by the model F-value, is generally lower than that of the double exponential decay function (Table 7). Figure 4 shows the deactivation fits for the three catalysts by the single exponential decay model. The underestimation of the initial activities is clearly illustrated in the figure.

4. Conclusion

The long-term deactivation of supported Pt catalysts in MCH dehydrogenation has been successfully included in the non-Langmuirian/noncompetitive Horiuti−Polanyi model. This has been accomplished by using the sum of two exponential decay functions to represent the fast and slow deactivation phases observed in the majority of tested catalysts. The work also indicates that an optimization of catalyst stability can be achieved by reducing the duration and sharpness of the fast deactivation phase, which allows the catalyst to operate at higher activity in the slow deactivation phase.

Literature Cited

(1) Alhumaidan, F.; Cresswell, D.; Garforth, A. Kinetic model of the dehydrogenation of methylcyclohexane over monometallic and bimetallic Pt catalysts. *Ind. Eng. Chem. Res.*, in press, DOI: 10.1021/ie100352p.

(2) Wolf, E. E.; Petersen, E. E. Kinetics of deactivation of a reforming catalyst during methylcyclohexane dehydrogenation in a diffusion reactor. *J. Catal.* **1977**, *46*, 190–203.

(3) Herz, R. K.; Gillespie, W. D.; Petersen, E. E.; Somorjai, G. A. The structure sensitivity of cyclohexane dehydrogenation and hydrogenolysis catalyzed by platinum single crystals at atmospheric pressure. *J. Catal.* **1981**, *67*, 371–386.

(4) Ngomo, H. M.; Susu, A. A. Investigation of prolonged deactivation-regeneration regimes on the dehydrogenation activity of platinum/alumina catalyst. *Pet. Sci. Technol.* **2001**, *19*, 283–298.

(5) Jossens, L. W.; Petersen, E. E. Fouling of a platinum reforming catalyst accompanying the dehydrogenation of methyl cyclohexane. *J. Catal.* **1982a**, *73*, 377–386.

(6) Pacheco, M. A.; Petersen, E. E. On a general correlation for catalyst fouling. *J. Catal.* **1984a**, *86*, 75–83.

(7) Pacheco, M. A.; Petersen, E. E. On the development of a catalyst fouling model. *J. Catal.* **1984b**, *88*, 400–408.

(8) Chai, M.; Kawakami, K. Kinetic model and simulation for catalyst deactivation during dehydrogenation of methylcyclohexane over commercial Pt, PtRe and presulfided PtRe-Al2O3 catalyst. *J. Chem. Technol. Biotechnol.* **1990**, *51*, 335–345.

(9) Corma, A.; Cid, R.; Agudo, A. Catalyst decay in the kinetics of methylcyclohexane dehydrogenation over Pt-NaY zeolite. *Can. J. Chem. Eng.* **1979**, *57*, 638.

(10) Davis, S. M.; Zaera, F.; Somorjai, G. A. The reactivity and composition of strongly adsorbed carbonaceous deposits on platinum. Model of the working hydrocarbon conversion catalyst. *J. Catal.* **1982**, *77*, 439–459.

(11) Doolittle, W. J.; Skoularikis, N. D.; Coughlin, R. W. Reactions of methylcyclohexane and n-heptane over supported Pt and Pt---Re catalysts. *J. Catal.* **1987**, *107*, 490–502.

(12) Biloen, P.; Helle, J. N.; Verbeek, H.; Dautzenberg, F. M.; Sachtler, W. M. H. The role of rhenium and sulfur in platinum-based hydrocarbon-conversion catalysts. *J. Catal.* **1980**, *63*, 112–118.

(13) Sachtler, W. M. H. Selectivity and rate of activity decline of bimetallic catalysts. *J. Mol. Catal.* **1984**, *25*, 1–12.

(14) Coughlin, R. W.; Kawakami, K.; Hasan, A. Activity, yield patterns, and coking behavior of Pt and PtRe catalysts during dehydrogenation of methylcyclohexane: I. In the absence of sulfur. *J. Catal.* **1984a**, *88*, 150–162.

(15) Coughlin, R. W.; Hasan, A.; Kawakami, K. Activity, yield patterns, and coking behavior of Pt and PtRe catalysts during dehydrogenation of methylcyclohexane: II. Influence of sulfur. *J. Catal.* **1984b**, *88*, 163–176.

(16) Jossens, L. W.; Petersen, E. E. Fouling of a platinum-rhenium reforming catalyst using model reforming reactions. *J. Catal.* **1982b**, *76*, 265–273.

(17) Pacheco, M. A.; Petersen, E. E. Reaction kinetics of methylcyclohexane dehydrogenation over a sulfided Pt + Re/Al2O3 reforming catalyst. *J. Catal.* **1985**, *96*, 507–516.

(18) Pal, A. K.; Bhowmick, M.; Srivastava, R. D. Deactivation kinetics of platinum-rhenium reforming catalyst accompanying the dehydrogenation of methylcyclohexane. *Ind. Eng. Chem. Process Des. Dev.* **1986**, *25*, 236–241.

(19) Van Trimpont, P. A.; Marin, G. B.; Froment, G. F. Kinetics of methylcyclohexane dehydrogenation on sulfided commercial platinum/alumina and platinum-rhenium/alumina catalyst. *Ind. Eng. Chem. Fundam.* **1986a**, *25*, 544–553.

(20) Alhumaidan, F. Hydrogen storage in liquid organic hydride: Producing hydrogen catalytically from methylcyclohexane. Ph.D. thesis, University of Manchester, Manchester, 2008.

(21) Horiuti, I.; Polanyi, M. Exchange reactions of hydrogen on metallic catalyst. *J. Chem. Soc., Faraday Trans.* **1934**, *30*, 1164.

(22) Augustine, R.; Van Peppen, J. Mechanistic comparison of heterogeneous and homogeneous hydrogenation. *Ann. N. Y. Acad. Sci.* **1969**, *158*, 482–491.

(23) Lin, S. D.; Vannice, M. A. Hydrogenation of aromatic hydrocarbons over supported Pt catalysts. I. Benzene hydrogenation. *J. Catal.* **1993**, *143*, 539–553.

(24) Lin, S. D.; Vannice, M. A. Hydrogenation of aromatic hydrocarbons over supported Pt catalysts. II. Toluene hydrogenation. *J. Catal.* **1993**, *143*, 554–562.

(25) Lin, S. D.; Vannice, M. A., III. Reaction models for metal surfaces and acidic sites on oxide supports. *J. Catal.* **1993**, *143*, 563–572.

(26) Thybaut, J.; Saeys, M.; Marin, G. Single-event microkinetics of aromatics hydrogenation on a Pt catalyst. AIChE Annual Meeting, San Francisco, CA, 2006.

Received for review June 17, 2010
Revised manuscript received August 9, 2010
Accepted September 1, 2010

IE1013025